# Energy Simulations of a Transparent-Insulated Office Façade Retrofit in London, UK

**I.L. Wong[1*], P.C. Eames[2], R.S. Perera[3]**

[1]*School of Engineering and Built Environment, Glasgow Caledonian University, 70 Cowcaddens Road, Glasgow, G4 0BA, UK (email: xijiayu@hotmail.com; IngLiang.Wong@gcu.ac.uk)*
[2]*CREST, Electronic and Electrical Engineering, Loughborough University, Leicester, LE11 3TU, UK (email: P.C.Eames@lboro.ac.uk)*
[3]*School of the Built and Natural Environment, Northumbria University, Newcastle upon Tyne, 115 Wynne-Jones Centre, NE1 8ST, UK (email: srinath.perera@northumbria.ac.uk)*

**Abstract**

Transparent Insulation Materials (TIMs) have been developed for application to building facades to reduce heating energy demands of a building. This research investigates the feasibility of TI-applications for high-rise and low-rise office buildings in London, UK, to reduce heating energy demands in winter and reduce overheating problems in summer. The energy performance of these office building models was simulated using an energy simulation package, Environmental Systems Performance-research (ESP-r), for a full calendar year. The simulations were initially performed for the buildings with conventional wall elements, prior to those with TI-systems (TI-walls and TI-glazing) used to replace the conventional wall elements. Surface temperatures of the conventional wall elements and TI-systems, air temperature inside the 20mm wide air gaps in the TI-wall, dry-bulb zone temperature and energy demands required for the office zones were predicted. Peak temperatures of between 50 and 70°C were predicted for the internal surface of the TI-systems, which clearly demonstrated the large effect of absorption of solar energy flux by the brick wall mass with an absorptivity of 90% behind the TIM layer. In the office zones, the magnitude of temperature swings during daytime was reduced, as demonstrated by a 10 to 12 hours delay in heat transmission from the external façade to the office zones. Such reduction indicates the overheating problems could be reduced potentially by TI-applications. This research presents the scale and scope of design optimisation of TI-systems with ESP-r simulations, which is a critical process prior to applications to real buildings.

Keywords: Transparent Insulation System; temperature profiles; energy simulation; building façades; London climate; energy demand

## 1 Introduction

The installation of opaque insulation with thickness of up to 50cm to building façades to reduce heat loss has been an issue for many building designers due to the resulting reduction of occupied space. The development of Transparent Insulation Materials (TIMs) for application to building façades not only responds to this issue, but also reduces heating energy demands of buildings. TIMs are small-celled honeycomb structures, made of highly transparent films, such as,

* Corresponding author; Tel: +44(0)1413313864; Fax: +44(0)1413313370

polypropylene, polycarbonate, polymethylmethacrylate (PMMA), translucent foam, and aerogels. Depending on the geometrical layout of the materials, TIMS can be classified into four generic types, such as, absorber-parallel, absorber-perpendicular, cavity and quasi-homogeneous structures (Wong *et al*., 2007). Each has a unique pattern of solar transmission and physical behaviour. Absorber-parallel and absorber-perpendicular structures, which comprise of multiple glazing elements or transparent plastic films parallel or perpendicular to the absorber surface, result in an increase in optical reflection or transmission. Cavity structures are the combination of absorber-parallel and absorber-perpendicular structures. Quasi-homogeneous structures include TIMs made of glass fibre or aerogel and are characterised by both scattering and absorption of incident radiation within the TIM. Examples of quasi-homogeneous structures are translucent plastic PTFE film (Chevalier et al., 1998) and translucent silica aerogels with 25-80% optical transparency for window application (Ackerman *et al*., 2001). TIMs can be applied to the building facades as TI-wall (wall) and TI-glazing (window) (see Figure 1). A TI-glazing system can be introduced when a layer of TIM is encapsulated between two glass panels; whilst, a TI-wall system requires a massive wall to be in place behind a TI-glazing as a thermal storage. For more than 20 years, TIMs have been used extensively for a range of building applications in mostly cold climatic regions to reduce building heating and lighting loads. TI-systems when used to replace standard opaque insulation materials, not only perform similar functions to opaque insulation, reducing heat losses and making indoor temperatures easier to control, but can allow solar transmittance of more than 50%. With a thickness of less than 20cm, it can provide a financial return to building occupants particularly, in urban areas, when it is applied to building facades, by maximising the occupiable and sell-able spaces, without compromising thermal comfort within buildings.

- insert Figure 1-

## 2 Research Background

For more than 20 years, TIMs have been used for various applications (Wong *et al*., 2005; Wong *et al*., 2007; Platzer, 2001). The earliest references relate to both theoretical and experimental work on the use of TIMs as aperture covers for flat-plate solar collectors (Hollands, 1965; Tabor, 1969; Symons, 1984; Hollands and Iynkaran, 1985; Platzer, 1987; 1992a; 1992b; Goetzberger, 1991; Goetzberger *et al*., 1992; Nordgaard and Beckman, 1992; Rommel and Wagner, 1992; Ghoneim, 2005). Later work introduce TIMs integrated into building façades to provide natural lighting and solar space heating to reduce lighting and heating energy demands in buildings (Voss *et al*., 1996; Wallner *et al*., 2004). TIMs can be used to replace conventional windows to provide TI-glazing; when TIMs are used to replace opaque insulation materials on a building exterior with the support of metal or wooden frames, a TI-wall can be formed (IEA,

1997). TIMs combine the advantages of opaque insulation and solar energy collection, the conductive heat losses through a building wall are reduced and solar radiation transmitted through the TIM can be converted into useful heat in the room or at the dark painted wall surfaces in TI-walls (Goetzberger, 1991). In 1982, the first real outdoor TI-wall experiments were undertaken by the Fraunhofer Institute for Solar Energy System (FISES) (Braun *et al*., 1992). Since then, a range of both experimental and theoretical studies on TIMs for building applications have been undertaken (Wallner *et al*., 2004; Wilke and Schmid, 1991; Twidell *et al*., 1994; Dalenback, 1996; IEA, 1997; Lien *et al*., 1997; Voss, 2000; Wong, 2007).

Computer simulation programs have been developed that predict the thermal and optical implications of integrating TI-systems to building façades before real systems are manufactured and installed (Braun et al., 1992; Wilke and Schmid, 1991; Sick and Kummer, 1992; Strachan and Johnstone, 1994; Manz *et al*., 1997; Matuska, 2000). In comparison to using scale-models, it is economic both in terms of time and finance to conduct simulations which permit parametric changes to TI-systems to be readily undertaken, enabling design optimisation guidance to be developed (Wong, 2007; Strachan and Johnstone, 1994). The daylighting and heating performance of buildings are strongly influenced by the employed TI-system parameters. The installation of an excessive quantity of TIMs is not only uneconomical, but can also cause problems of overheating. Many building simulation programs and modelling approaches have been adapted and employed to simulate TI-applications, particularly, WANDSIM (Wilke and Schmid, 1991), TRNSYS (Sick and Kummer, 1992), HAUSSIM (Braun *et al*., 1992), and Environmental Systems Performance – research (ESP-r) (Wong, 2007; Strachan and Johnstone, 1994; Matuska, 2000; Heim, 2004). From all the available software, ESP-r (ESRU, 2002) has been widely used and is available to undertake simulations of various types of building with complex zones and thermal control systems (Wong *et al*., 2008; Jenkins *et al*., 2009a; Jenkins *et al*., 2009b; Spindler and Norford, 2009; Høseggen *et al*., 2009).

## 3 Energy Simulations of Office Buildings with TI-façades

This research aims to investigate the suitability of applying TI-wall and TI-glazing to the high-rise and low-rise office buildings in London, UK, to reduce heating energy demands during winter and to study the potential of reducing overheating during summer. Simulations were initially performed to assess the energy performance of the office buildings with conventional building facades. The simulations were repeated with the use of transparent insulated building façades used to replace the conventional facades. Due to its ability to simulate the energy performance of complex building models with integrated TIMs and perform detailed airflow analysis (Wong et al., 2007), ESP-r was selected to undertake the building energy simulations. To reduce the complexity of the simulations, only zones on

ground, middle and top floors were modeled for high-rise building; whilst for low-rise building, ground and top floors were simulated (Figure 2~~Figure 2~~). London climatic data (hourly values) available from the ESP-r database was used. Using ESP-r, different patterns of heating and cooling in the buildings were defined; whilst, occupancy patterns, infiltration and ventilation rates were assumed to meet standard requirement for office buildings in the UK. Sensible and latent heat emitted from occupants and electrical appliances in the buildings were defined. In ESP-r, the integration of a TIM into a building facade can be simulated by creating a separate thermal zone as an air gap between the brick wall mass and the TI-system. Surface temperatures of different layers of building façades and the south facing office zone temperature were predicted; and the energy demands required to maintain the comfort temperature within the office buildings were also predicted.

### *3.1 Generic Types of Office Buildings*

Energy performance simulations were performed for two generic types of high-rise and low-rise office building (Figure 2) using London climatic data. As indicated in Table 1, the 15-storey high-rise office building chosen had a rectangular cross-section 35m x 15m and a gross floor area (GFA) of 7875m$^2$. It was stand-alone, with none of the surrounding buildings connected to it and most of the north and south facing façades were external windows. The total areas of external wall and windows were set to be 2943 m$^2$ and 1536 m$^2$. The low-rise, 15m x 10m, rectangular 4-storey office building had two office rooms, a store room, and a lavatory on each floor. It has a GFA of 600m$^2$, external wall and window areas of 510m$^2$ and 85m$^2$. Its west and east sides were attached to the surrounding buildings which were of similar height, thus external façades and windows are only available in two directions. Both types of building had 3m floor to floor height. The footprints of these two types of office building were chosen because most office buildings in UK urban areas are of similar dimensions. The stand alone high-rise office building model can be used to represent office block in the UK cities, particularly, London. The low-rise office building model (terrace building) is a common sight in most UK urban and sub-urban areas. The internal layout and types of building services used in these buildings were also assumed to be similar to those used in the standard office buildings in the UK.

-insert Figure 2-

-insert Table 1-

Simulation domains were created for both types of the office buildings as illustrated in Figure 3~~Figure 3~~ and Figure 4~~Figure 4~~, which indicate the layout plans of the simulated building zones on different floors and the building parameters. Simulated building zones are defined in Table 2. The building dimensions were entered into ESP-r as grid points, which consist of vertices (x, y, z) to represent building length, width and height. The high-rise and low-rise

office buildings had a grid of 35.0 x 15.0 and 15.0 x 10.0 points, respectively, which were used to reflect the building dimensions. Each grid point was unique and was required for accurate calculations to avoid confusion, particularly, for the calculations of small dimensions.

-insert Figure 3-

-insert Figure 4-

-insert Table 2-

*3.2 Types of Building Facades*

Two types of conventional building façades considered were cavity wall with opaque insulation (U-value: 0.35W/$m^2$K) and double-glazed windows (U-value: 2.78W/$m^2$K), as indicated in Figure 5 (i & ii). These building materials were assumed to be the original building facades of the buildings. Brickwork was chosen for the base case building facade construction because it is a commonly used building material that is used in many countries for many types of buildings. Despite no official statistical data showing the percentage of office buildings constructed with external brick walls in the UK, most post-war buildings in the UK were built using bricks (Campbell, 2003).

-insert Figure 5-

For the simulations, the buildings were retrofitted, with TI-wall and TI-glazing (Figure 5v & vi) used to replace the conventional façades on the south facing building facades. The TI-system used was the KAPILUX System (U-value: 1.34W/$m^2$K) manufactured by OKALUX GmbH in Germany, which consisted of a layer of TIM, PMMA encapsulated inside a double-glazed unit. The TI-wall was constructed by applying the TI-system to the external surface of a brick wall, with a 20mm wide air gap in between the TI-system and the wall. The brick wall was approximately 300mm thick with a U-value of 1.87W/$m^2$K and a density of 2000kg/$m^3$, its external surface was blackened and had an absorptivity of 0.9. The type of glass used to manufacture the window glazing was clear soda-lime float glass. For ESP-r, TI-systems can be modelled as a transparent multilayer construction, where, each layer of the TI-system is explicitly simulated, with conduction, convection and radiation occurring (ESRU, 2002). For a TI-wall, the heat absorbed in the TI-system was subsequently transferred to the air gap by convection. For TI-system simulation, specific optical properties, such as, direct transmission and the absorption in each layer of the system were calculated for five different angles of incidence (0°, 40°, 55°, 70° and 80°) using numerical models developed by Wong and Eames (2011). The values were used to populate databases required by ESP-r for simulation of the TI-System. Table 3 indicates the thermo-physical and optical

properties for the surfaces in the simulated building models. For each surface of the building models, boundary conditions were defined and applied to the building facades.

-insert Table 3-

### *3.3 Four Building Envelope Configurations*

Simulations were undertaken using ESP-r for four different building envelope arrangements, designated as Cases 1, 2, 3 and 4. As illustrated in Figure 6, Case 1 was the base case simulation, being for a conventional building envelope currently used for commercial buildings, whereas, in Cases 2, 3 and 4, TI-façades were used to replace the south facing conventional façades of the office buildings. In Case 2, the south facing double-glazed windows in the office zones of the office buildings were replaced with TI-glazing units. In addition to that, two TI-wall units with 20mm air gaps were also integrated into the external cavity wall. In Case 3, the simulations were repeated with only TI-glazing integrated into the south facing façades of the office zones, replacing the TI-wall described in Case 2. In Case 4, the simulations were repeated for building facades identical to those used in Case 2, with the 20mm air gap between the TI-System and the brick wall mass was reduced to minimum (1 mm). This was done to investigate the effects of air gap reduction on the energy performance of the TI-system. In all simulations, the construction materials used for floor slab, roof slab and internal walls were maintained and only the external cavity walls and double-glazed windows were modified by using different types of façade and construction materials.

-insert Figure 6-

### *3.4 Meteorological Data*

The weather data was obtained from the US Department of Energy website, which can be imported to and converted by ESP-r. The data was from the International Weather for Energy Calculations (IWEC), which is in EPW data and used by EnergyPlus. The file supports hourly data and includes diffuse and direct solar intensities, external dry-bulb temperature, relative humidity and wind speed. The hour-by-hour weather data of a typical meteorological year for London, UK (Figure 7) was used for the simulations. The simulations were conducted for the entire calendar year and the results of weekly time periods for the four different seasons were extracted: January ($2^{nd}$ to $8^{th}$), April ($1^{st}$ to $7^{th}$), July ($12^{th}$ to $18^{th}$) and December ($1^{st}$ to $7^{th}$). The simulation periods selected contain either maximum or minimum ambient temperatures in the year and thus provide a basis for comparing the performance of the simulated buildings under extreme ambient temperatures. The highest air dry-bulb temperature simulated during summer was 27.7˚C at 12:00 on the $17^{th}$ of July, the minimum temperature of -6.4˚C was recorded at 20:00 on the $8^{th}$ of January, with the

highest intensities of direct and diffuse solar radiation (Figure 8) were simulated in spring and summer (March to September).

-insert Figure 7-

-insert Figure 8-

### *3.5 Heating and Cooling Controls*

The patterns of heating and cooling in the building models were defined to reflect realistic environmental controls and to achieve thermal comfort in the office buildings. An auxiliary heating or cooling systems was activated one hour before the start of the working day at 08:00 on a lower heating set point and at half of the full capacity and operated at maximum capacity during office hours (09:00 to 17:00). Heating and cooling capacities varied from 0 to 23kW depending on the size of the office zones and these set points and are indicated in Table 4. When the buildings were unoccupied, heating and cooling system controls were set to free-floating, whilst, during working hours, the controls were activated when the air temperature dropped below or exceeded the defined heating or cooling set point. Heating and cooling set points were 20˚C and 24˚C respectively, in order to maintain thermal comfort (between 20˚C and 25˚C) inside the office zones.

-insert Table 4-

### *3.6 Occupancy Patterns*

Occupancy patterns are defined to allow accurate and realistic predictions to reflect real building operations. It was assumed that, the occupancy rate of the office buildings was approximately 10 to 15$m^2$ floor area per person (ESRU, 2002; BSJ, 2005).

### *3.7 Infiltration and Ventilation*

CIBSE (2007) reported a mechanical ventilation rate of 1.65 air changes per hour (ACH) for air conditioned office buildings of up to 16 storeys to comply with the Building Regulations. It does not however specify detailed rates for different zones in the office buildings. Thus, for all zones, a rate from 0.5 to 1.5 ACH was applied, which complies with the requirements for office buildings (CIBSE, 1986; 2007; BSJ, 2004). A rate of 10 ACH was applied to office zones, lavatories and corridors when the internal air temperature exceeded 20°C and was varied according to the types of activities undertaken in the rooms.

### *3.8 Internal Heat Gains*

It was assumed that standard office electrical appliances, such as, computers, fax machines, printers, photocopy machines and video conferencing facilities were used in the buildings. The artificial lighting systems used were of the tubular fluorescent type, supplying 300 to 400lux illumination to comply with the illumination levels required for a standard office building of between 250 and 500lux (Dubois, 2003; Serra, 1998). The sensible and latent heat emitted from the occupants were assumed to be 90 and 50W per occupant (CIBSE, 1986; 2007), 10 and 5W per $m^2$ from lighting (CIBSE, 1986; 2007), and 45 and 25W per $m^2$ from electrical appliances (ESRU, 2002). Lights were switched on one hour before the working day and switched off at 19:00 in all occupied zones. Electrical appliances, such as, computers, printers and copy machines were assumed to operate during working hours only and to be switched off after this. The internal heat gains vary according to the building occupancy and multiple studies on the impact of the behaviour of occupants on buildings' energy demands have been conducted by various researchers, such as, Mahdavi (2009), Haldi and Robinson (2010) and Haldi *et al*., (2010). Previous findings on internal heat gains or occupancy rate during lunch break are inconsistent and contradicteach other, with values ranging from 20% (Saelens *et al*., 2011) to 80% (Winkelmann *et al*., 1993) for office buildings. Thus, this study used an average occupancy rate of 50% for the office rooms during the lunch break (12:00 to 14:00).

## 4 Prediction of Surface Temperature

The surface temperatures of the four types of building façades were predicted at the different locations, as demonstrated in Figure 9. Initial simulations of office zones on different floors indicated that the patterns of temperature distribution on the lower, intermediate and top floors were similar with average temperature differences of less than 2°C. To reduce complexity and the amount of simulations undertaken, only office zones, corridors and lavatories on the ground floor were modelled and the results were used to represent the performance of zones on other floors.

-insert Figure 9-

The surface temperature profiles for all types of south facing building façades [Cases 1 (C1) to 4 (C4)] in the office zones of the high-rise and low-rise office buildings are predicted. Figure 10 and Figure 11 illustrate the predicted façade surface temperatures for the high-rise office building in winter ($2^{nd}$ and $3^{rd}$ of January) and summer ($12^{th}$ and $13^{th}$ of July), respectively. The surface temperature difference of TI-wall with 20mm air gap (C2) and with minimum thickness of air gap (C4) was less than 1°C. These simulations indicate that, variation to the thickness of air gap between TI-system and the brick wall has insignificant impact on the energy performance of the TI-wall, demonstrated by the C2 graph overlapped with the C4 graph. Surface temperatures of building façades were generally higher than ambient

temperature and varied with time, this was due to the solar radiation absorbed at these surfaces. The large increase in surface temperature was predicted due to the amount of direct solar radiation absorbed during the day.

-insert Figure 10-

In the high-rise office building, the internal surface temperature of the TI-glazing (C3) exceeded 29°C at noon, despite the ambient temperature being close to the freezing point in winter (Figure 10a). This was due to the maximum direct solar radiation of more than 500W/$m^2$ predicted at that time. The higher surface temperature predicted at TI-glazing (C3) compared to those predicted at the double glazing (C1) demonstrates the effect of solar energy flux absorbed. When the TI-wall was simulated (C2), a peak temperature of more than 48°C was predicted at noon (Figure 10b), the result of incident direct radiation intensities of more than 500W/$m^2$. Subsequently, increasing temperatures were predicted at the external (16:00) and internal (up to 00:30) surfaces of the brick wall mass, indicating transmission of the incident solar energy flux from the TI-System to the brick wall mass. The heat flux absorbed and stored in the brick wall mass was released to the office zones through convective heat transfer at night, when the ambient temperature was close to zero. A delay of approximately 6 to 12 hours was predicted for the energy flux to be transmitted from the TI-system to the internal surface of the brick wall mass, this may help to minimise overheating problems in the office zones at mid day. The patterns of surface temperature distribution predicted for the low-rise office building were very similar to those predicted for the high-rise office building because the types of building façade used in both office buildings were similar with the same physical and optical properties.

-insert Figure 11-

In summer (Figure 11), surface temperatures predicted for all cases were generally higher than the temperatures predicted in winter due to higher solar energy flux and increased ambient temperature. On the 12$^{th}$ of July, incident solar radiation intensities of more than 300W/$m^2$ were predicted for a total of nine hours (07:00 to 16:00), compared to five hours (10:00 to 15:00) predicted on the 2$^{nd}$ of January. For TI-wall application (C2), temperatures of more than 70°C were predicted at the internal surface of the TI-System at 15:00 (Figure 11b). The heat flux was then transmitted from the TI-System to the brick wall mass, indicated by the subsequent peak temperatures predicted at the external and internal surfaces of the wall mass in the space of 10 to 12 hours. The prediction indicates the potential of reducing the magnitude of temperature swings and overheating problems during the day in summer.

It can be concluded that, the predicted surface temperatures for the TI-systems (C2, 3 and 4) were generally higher than for the standard façade on sunny days, due to the high absorptivity (90%) of the TIM and brick wall mass. The TI-

systems absorbed more solar energy flux which is needed for space heating in winter, compared to conventional building facades. When solar radiation was absorbed in the day by the TI-systems, the solar energy flux was transferred to the internal layers of the system, as indicated by the subsequent surface temperature rise from external to internal surfaces of the TI-wall, The application of the brick wall mass behind the TI-systems (C2 and 4) stored and then released the heat flux to the office zones after 10 to 12 hours time lag. This significantly reduces the magnitude of temperature swings in the office zones. In summer, despite this temperatures exceeding 70°C were predicted at the internal surface of the TI-System in the afternoon (Figure 11), the energy was transmitted and absorbed by the brick wall mass and reduced overheating problems in the office zones. The delay in energy absorbed and transmitted by the brick wall mass can be seen by the peak temperatures at the external and internal brick wall mass surfaces being predicted to occur at 17:00 and 00:30.

## 5 Prediction of Zone Temperatures

The temperatures of the office zones and the air gap within the TI-wall in the high-rise and low-rise office buildings were predicted for winter and summer periods. Significant air gap temperature rises were predicted after the heating and cooling systems were switched off after office hours, due to the release of absorbed heat flux from the wall mass (discussed in previous section). Figure 12 indicates office zone temperatures during the cold winter period, where a rapid increase of office zone temperature at around 08:00 on the 2$^{nd}$ and 3$^{rd}$ of January was predicted, due to auxiliary heating. The office zones were heated until the zone temperature stabilised at the heating set point (20°C) at around 10:30. The temperature was then kept constant at this point to maintain the desired thermal comfort temperature in the office zones. The auxiliary system was switched-off after working hours (17:00). The solar radiation absorbed at the external façade surface was transmitted through the building facade and heat subsequently released into the office zone, which is shown by the higher zone temperatures predicted in the office zones. The highest zone temperatures are predicted to occur at night and are consistent with the predicted surface temperatures discussed previously, which indicate a delay of approximately 10 to 12 hours in the transmission of heat to the office zones.

-insert Figure 12-

In summer (Figure 13), auxiliary cooling was required for the office zones to maintain the comfort conditions, due to heating that occurred as a result of solar energy flux transmitted through the building facades and the internal casual gains. For sunny days with strong direct solar radiation, the zone temperatures were decreasing after cooling system was activated during the office hours and reached cooling set point of 24°C from 10:00 to 17:00. At the same time, solar energy flux was also absorbed by the wall mass. When the auxiliary cooling system was switched off after working

hours, the heat flux was released to the office zones between 18:00 and 00:00, which is consistent with the surface temperatures predicted in the previous section. Zone temperatures of up to 40°C were predicted due to heat release from the building facade to the zone, because the buildings were unoccupied and all lighting and electrical appliances were not in operation after working hours.

-insert Figure 13-

The simulations indicate that, zone temperatures in the office zones with TI-facades (C2 to C4) were generally 2 to 3°C higher than those with conventional façades (C1), which indicate increased solar energy gains resulting from the TI-application. The solar energy gains will not only reduce heating demand of the office zones during winter, but also stabilise the zone temperatures during the day in summer, due to the wall mass. Figure 14 shows the air temperature profile inside the 20mm air gap of the TI-wall (C2) in winter (2$^{nd}$ and 3$^{rd}$ of January) and summer (17$^{th}$ and 18$^{th}$ of July). The prediction indicates a steep rise in air gap temperature during the day, with a maximum temperature of 65°C was predicted in summer. Despite, the ambient temperature being close to 0°C in winter, the air gap temperature was near to 45°C in the afternoon, demonstrating the effect of solar energy absorption by the TI-System. This result agrees well with the surface and office zone temperature profiles predicted.

-insert Figure 14-

## 6 Prediction of Annual Energy Demands

The annual energy demands were defined as the energy required to achieve the heating and cooling set point temperatures in the south facing office zones of the office buildings. The energy demands required for both high-rise and low-rise office buildings for different seasons in a full calendar year were predicted. Heating dominates during the winter months (from October to March), with up to 1164 heating hours (C1); whilst for the TI-application, the minimum heating hours were down to 973 hours (C3). The annual heating energy demands required for both office buildings (between 32 and 44kWh/m$^2$) with TI-application (C2 to C4) were 6 to 8% less than those with conventional facades (C1) (between 35 and 47kWh/m$^2$). The application of TI-facades however, had contributed to additional cooling energy demands during the summer months (from April to September), demonstrated by an increase in cooling hours of approximately 150 hours (C3).

## 7 Reduction of Overheating Problems with the Applications of Overhangs and Natural Ventilation

To reduce the overheating problems due to TI-applications, the simulations were repeated with external overhangs and air vents (Figure 15~~Figure 15~~) applied to the upper section of the TI-façades. The overhangs simulated had four depths

(0.8, 1.0, 1.2 and 1.5m) and could be constructed using a 70mm thick conventional reinforced concrete slab, horizontally (90°) positioned to the vertical external wall to provide shading to incoming solar radiation. The air vents used in the simulations were similar to the type used in a traditional trombe wall. The air vents allow the office zones to be naturally ventilated to achieve the thermal comfort temperature (20 to 25°C), instead of using a mechanical cooling system and eliminated the cooling energy demands in these zones. For the simulations, the air vents (with a total area of either 2 or 4$m^2$) were opened during summer (from the 1st of June to the 30th of September); and sealed during winter (from the 1st of October to the 31st of May), to prevent the cold ambient air from entering the office zones. The office zones were naturally ventilated either 24 hours per day or during office hours only (from 09:00 to 17:00) at a 20°C set point temperature, to allow the free flows of natural air into the south facing office zones with TI-façades. The heating and cooling energy demands required for the office zones with overhangs and air vents were simulated.

-insert Figure 15-

Initial simulations indicate that, a further increase in the depth of the overhangs from 0.8 to 1.5m contributed an insignificant additional cooling effect. Thus, optimum cooling performance was predicted when 0.8 or 1m deep overhangs were applied to the TI-façades. Figure 16~~Figure 16~~ indicates an extract from zone temperature simulations for a high-rise office zone, either mechanically or naturally ventilated with 0.8m deep overhangs in the London climate. For mechanically ventilated office zones, the mechanical cooling system was activated to achieve the cooling set point temperature (24°C) during office hours (09:00 to 17:00). After office hours (17:00), the mechanical cooling system was switched off, which resulted in the air temperature increasing to more than 38°C inside the office zone, due to the release of heat from the building facades to the office zone. The simulations were repeated, with the office zone naturally ventilated. The air temperature in the office zone rose up to 28°C after 12:30, due to the increase in ambient temperature. Natural ventilation continued to create a cooling effect to maintain the zone temperature at less than 23°C after office hours. At 12:30 when the ambient temperature was 27.7°C, the air temperature in the naturally ventilated zone was slightly higher (27.96°C) than the ambient temperature. Compared to the mechanically ventilated office zone, the predicted air temperature in the naturally ventilated zone at 09:30 and 17:30 was 2 to 4°C lower. The zone temperature predicted with the 4$m^2$ air vents was 1 to 2°C lower than those with the 2$m^2$ air vents. When the office zone was naturally ventilated all day, the zone temperature was 1 to 2°C lower than those with natural ventilation occurred during office hours only. These simulations indicate that, significant overheating problems can be reduced in the naturally ventilated office zones without the aid of mechanical cooling, despite high ambient temperatures.

-insert Figure 16-

To achieve optimum energy saving, 0.8 to 1m deep overhangs and 4m$^2$ air vents were applied. The energy demands were converted into monetary values for comparison and the prices of fuels were calculated in accordance with the DTI (2005) (1.885 pence per kWh for gas and 5.95 pence per kWh for electricity). As illustrated in Table 5~~Table 5~~, annual energy demands predicted in the high-rise office building with the south facing TI-façades, combined with all day natural ventilation through 4m$^2$ air vents and 0.8 or 1m deep overhangs were 2.5% lower than those in Case 1 in London climate. In the low-rise office building with the application of natural ventilation and overhangs, energy savings of up to 2.6% were predicted. The minimum total energy demands were predicted in both high-rise and low-rise office buildings with the south facing TI-façades (Case 3), combined with 0.8 or 1m deep overhangs and 4m$^2$ air vents.

-insert Table 5-

## 8 Discussion

Simulations indicate that, for all office buildings, the surface temperatures of building façades were strongly affected by the amount of direct solar radiation absorbed. The TI-System and blackened brick wall mass used for the TI-wall with an absorptivity of 90% led to the highest surface temperatures. On a sunny afternoon in summer, temperatures of up to 80°C were predicted at the internal surface of the TI-System within a TI-wall. Subsequent peak surface temperatures were predicted at the external and internal surfaces of the brick wall mass in the evening and at midnight, approximately 10 to 12 hours after the prediction of the peak temperature at the TIM surface, which indicates a delay in energy transmission from the TI-System to the office zones. When the thickness of air gap inside the TI-wall was reduced from 20mm to 1mm, it had little effect on the energy performance of the office zone, as indicated by the identical surface temperatures predicted for the TI-walls and office zone temperatures for both C2 and C4. Despite ambient temperatures of less than 3°C, an average zone temperature of above 10°C was predicted in winter for all cases. The overall office zone temperature with a standard building façade (C1) was 1 to 2°C lower than those with the TI-application (C2 to C4). For all simulation cases, internal casual gains, heating and cooling control set points were assumed to be identical. The simulated results therefore demonstrate that, the increased surface and zone temperatures predicted in C2 to C4 were due to the additional solar energy gains as a result of the TI-application.

This paper clearly demonstrates the suitability of applying TIM to the south facing external facades of office buildings to reduce heating energy demands, albeit potential overheating problems occur during summer which could lead to an additional cooling requirement. The overheating problem however, could be minimised using increased brick wall mass and the application of overhangs and natural ventilation techniques. These simulations indicate that, overhangs and air vents can be integrated into TI-facades to provide solar shading and natural ventilation to the buildings, which can

reduce the cooling energy demands significantly. The study also indicates that, optimum energy savings could be achieved when the 0.8 to 1m deep overhangs and $4m^2$ air vents were applied. The application provides a cheaper alternative to the standard mechanical roller blinds used in previous research, which require regular maintenance. The simulations predicted both temperature profiles and energy demands of the office buildings. The effects of a TI-façade on artificial lighting energy demands, however, were not considered due to the fact that, ESP-r is not capable of conducting detailed simulations on the effects of the application of TI-façade to the lighting energy demands in a building. This is an important area and should be addressed in future work. The simulation results can also be validated if TI-systems are integrated in real building facades enabling experimental works to be undertaken and real time measurement data generated that can be used for comparison with the simulation results.

## 9 Conclusions

Surface temperatures of building facades and the air gap temperature inside the TI-wall were affected by the direct solar radiation absorbed at the building facade; whilst, the office zone temperature was affected by the heat released from the internal casual gains, the auxiliary heating and cooling systems and solar energy gains. The application of TI-façades to both types of office buildings has increased solar energy gains to the buildings, and the annual heating energy loads required can be reduced by up to 8%. The solar energy gains demonstrated due to TI-applications are consistent with previous studies. During summer, increased overheating problems may result due to the use of TI-façades, though with the application of a 300mm thick brick wall mass to a TI-system, the overheating problems were reduced and delayed by up to 12 hours in the office zones. It can be concluded that, TI-systems are highly suited to south facing external facade application in office buildings, having the potential to significantly reduce heating energy loads in winter and when combined with brick wall mass, natural ventilation and overhangs, overheating problem, in summer. This research investigates the feasibility of applying TI-systems to office building facades because previous TI-applications have been focused on low-rise and non office buildings only. This study was the first of its kind, undertaken to investigate and compare the performance of TI-facades in low-rise and high-rise office buildings. This research provides details of design optimisation of TI-façades in office buildings with ESP-r simulations, which is a critical process prior to applications to real buildings.

**Acknowledgements**

The authors would like to express their gratitude to OKALUX GmbH for the TI-System product information. A University of Ulster research studentship is hereby acknowledged by the first author.

**References**

(2004), “Rules of thumb – comfort factors”, *Building Services Journal*, Vol. 26 No. 2, pp. 22-23.

(2005), "Wellcome home", *Building Services Journal*, Vol. 27 No. 2, pp. 26-30.
Ackerman, W. C., Vlachos, M., Rouanet, S., and Fruendt, J. (2001), "Use of surface treated aerogels derived from various silica precursors in translucent insulation panels", *Journal of Non-Crystalline Solids*, Vol. 285, pp. 264-271.
Braun, P.O., Geotzberger, A., Schmid, J. and Stahl, W. (1992), "Transparent insulation of building facades – steps from research to commercial applications", *Solar Energy*, Vol. 49 No. 5, pp. 413-427.
Campbell, J.W.P. (2003), *Brick: A world history*, Thames & Hudson Ltd: London.
Chevalier, B., Hutchins, M.G., Maccari, A., Olive, F., Oversloot, H., Platzer, W., Polato, P., Roos, A., Rosenfeld, J. L. J., Squire, T., and Yoshimura, K. (1998), "Solar energy transmittance of translucent samples: A comparision between large and small integrating sphere measurements", *Solar Energy Materials and Solar Cells*, Vol. 54, pp. 197-202.
CIBSE (1986), *CIBSE Guide A4: Air Infiltration and Natural Ventilation, Volume A: Design Data, 5th edition*, CIBSE, London.
CIBSE (2007), *CIBSE Guide A: Environmental Design, 7th Edition, Issue 2*, The Chartered Institution of Building Services Engineers, London.
Dalenback, J-O. (1996), "Solar energy in building renovation", *Energy and Buildings*, Vol. 24 No. 1, pp. 39-50.
Department of Trade and Industry (DTI) (2005), *DTI Quarterly Energy Prices September 2005, Prices of fuels purchased by non-domestic consumers*.
Dubois, M-C. (2003), "Shading devices and daylight quality: an evaluation based on simple performance indicators", *Lighting Research Technology*, Vol. 35 No. 1, pp. 61-76.
ESRU. (2002), *The ESP-r System for Building Energy Simulation, User Guide Version 10 Series, ESRU Manual U02/1*, Energy Systems Research Unit, University of Strathclyde.
Ghoneim, A.A. (2005), "Performance optimisation of solar collector equipped with different arrangement of square-celled honeycomb", *International Journal of Thermal Sciences*, Vol. 44, pp. 95-105.
Goetzberger, A. (1991), *Transparent insulation technology for solar energy conversion*, 2nd Edition, Fraunhofer Institute for Solar Energy Systems, Freiburg.
Goetzberger, A., Dengler, J., Rommel, M., Gottsche, J. and Wittwer, V. (1992), "A new transparently insulated, bifacially irradiated solar flat-plate collector", *Solar Energy*, Vol. 49 No. 5, pp. 403-411.
Haldi, F. and Robinson, D. (2010), "The impact of occupants'behaviour on urban energy demand", *in Proceeding of the Third German-Austrian IBPSA Conference*, 22-24 September 2010, Vienna University of Technology.
Haldi, F., Robinson, D., Pröglhöf, C. and Mahdavi, A. (2010), "The double blind evaluation of a comprehensive window opening model", *in Proceeding of the Third German-Austrian IBPSA Conference*, 22-24 September 2010, Vienna University of Technology.
Heim, D. (2004), "Whole year analysis of TIM-PCM solar thermal storage wall", *in Proceeding of the SimBuild 2004, IBPSA-USA National Conference, August 4-6*, Boulder CO, USA.
Hollands, K.G.T. (1965), "Honeycomb devices in flat plate solar collectors", *Solar Energy*, Vol. 9 No. 3, pp. 159-164.
Hollands, K.G.T. and Iynkaran, K. (1985), "Proposal for a compound-honeycomb collector", *Solar Energy*, Vol. 34 No. 4-5, pp. 309-316.
Høseggen, R., Mathisen, H.M. and Hanssen, S.O. (2009), "The effect of suspended ceilings on energy performance and thermal comfort", *Energy and Buildings*, Vol. 41 No. 2, pp. 234-245.
IEA (1997), *IEA Solar Heating and Cooling Programme, Task 20: Solar Energy in Building Renovation*, James and James Ltd, London.
Jenkins, D.P., Peacock, A.D. and Banfill, P.F.G. (2009a), "Will future low-carbon schools in the UK have an overheating problem?", *Building and Environment*, Vol. 44 No. 3, pp. 490-501.
Jenkins, D.P., Singh, H. and Eames, P.C. (2009b), "Interventions for large-scale carbon emission reductions in future UK offices", *Energy and Buildings*, Vol. 41 No. 12, pp. 1374-1380.
Lien, A.G., Hestnes, A.G. and Aschehoug, O. (1997), "The use of transparent insulation in low energy dwellings in cold climates", *Solar Energy*, Vol. 59 No. 1-3, pp. 27-35.
Mahdavi, A. (2009), "Patterns and Implications of User Control Actions in Buildings", *Indoor and Built Environment*, Vol 18 No. 5, pp. 440-446.
Manz, H., Egolf, P.W., Suter, P. and Goetzberger, A. (1997), "TIM-PCM external wall system for solar space heating and daylighting", *Solar Energy*, Vol. 61 No. 6, pp. 369-379.
Matuska, T. (2000), "A simple trombe wall: comparison of different glazings", *in Proceedings of the ISES Congress EuroSun2000*, Copenhagen, 2000.
Nordgaard, A. and Beckman, W.A. (1992) "Modelling of flat plate collectors based on monolithic silica aerogel", *Solar Energy*, Vol. 49 No. 5, pp. 387-402.
Office of the Deputy Prime Minister (2006), *The Building Regulations 2000: Conservation of Fuel and Power, Approved document L2A: Conservation of fuel and power in new buildings other than dwellings, 2006 Edition*, NBS, London.

Platzer, W.J. (1987), "Solar transmittance of transparent insulation materials", *Solar Energy Materials*, Vol. 16, pp. 275-287.
Platzer, W.J. (1992a), "Directional-hemispherical solar transmittance data for plastic type honeycomb structures", *Solar Energy*, Vol. 49 No. 5, pp. 359-369.
Platzer, W.J. (1992b), "Total heat transport data for plastic honeycomb-type structures", *Solar Energy*, Vol. 49 No. 5, pp. 351-358.
Platzer, W.J. (2001), "Transparent insulation materials and products: a review", *Advances in Solar Energy*, Vol. 14, pp. 33-65.
Rommel, M. and Wagner, A. (1992), "Application of transparent insulation materials in improved flat-plate collectors and integrated collector storages", *Solar Energy*, Vol. 49 No. 5, pp. 371-380.
Saelens, D., Parys, W. and Baetens, R. (2011), "Energy and comfort performance of thermally activated building systems including occupant behaviour", *Building and Environment*, Vol. 46 No. 4, pp. 835-848.
Serra, R. (1998), "Chapter 6 – Daylighting", *Renewable and Sustainable Energy Review*, Vol. 2 No. 1-2, pp. 115-155.
Sick, F. and Kummer, J.P. (1992), "Simulation of transparently insulated buildings", *Solar Energy*, Vol. 49 No. 5, pp. 429-434.
Spindler, H.C. and Norford, L.K. (2009), "Naturally ventilated and mixed-mode buildings – Part I: Thermal modelling", *Building and Environment*, Vol. 44 No. 4, pp. 736-749.
Strachan, P.A. and Johnstone, C.M. (1994), "Solar residence with transparent insulation: predictions from a calibrated model", *in Proceedings of the North Sun 94*, Glasgow, 1994, pp. 347-353.
Symons, J.G. (1984), "Calculation of the transmittance-absorptance product for flat-plate collectors with convection suppression devices", *Solar Energy*, Vol. 33 No. 6, pp. 637-640.
Tabor, H. (1969), "Cellular insulation (honeycombs)", *Solar Energy*, Vol. 12 No. 4, pp. 549-552.
Twidell, J.W., Johnstone, C., Zuhdy, B. and Scott, A. (1994), "Strathclyde University's passive solar, low-energy, residences with transparent insulation", *Solar Energy*, Vol. 52 No. 1, pp. 85-109.
Voss, K. (2000), "Solar energy in building renovation – results and experience of international demonstration buildings", *Energy and Buildings*, Vol. 32 No. 3, pp. 291-302.
Voss, K., Braun, P.O. and Russ, C. (1996), "Transparent insulation in building renovation: German contribution to IEA-SHCP Task 20", *in Proceedings of the EuroSun'96*, Glasgow, pp. 1808-1812.
Wallner, G.M., Lang, R.W., Schobermayr, H., Hegedys, H. and Hausner, R. (2004), "Development and application demonstration of a novel polymer film based transparent insulation wall heating system", *Solar Energy Materials and Solar Cells*, Vol. 84 No. 1-4, pp. 441-457.
Wilke, W.S. and Schmid, J. (1991), "Modelling and simulation of elements for solar heating and daylighting", *Solar Energy*, Vol. 46 No. 5, pp. 295-304.
Winkelmann, F.C., Birdsall, B.E., Buhl, W.F., Ellington, K.L. and Erdem, A.E. (1993), *DOE-2 Supplement, Version 2.1E*, Lawrence Berkeley National Laboratory, Berkeley, California, LBL-34947, November.
Wong, I.L. (2007), *Optimum and cost effective transparent insulation systems for office building applications in temperate and tropical climates*, Ph.D. Thesis, School of the Built Environment, University of Ulster.
Wong, I.L. and Eames, P.C. (2011), "The development of numerical models to calculate the optical properties of a transparent insulation system", *in Proceedings of the International Conference on Harnessing Technology*, Muscat, Oman, 2011.
Wong, I.L., Eames, P.C. and Perera, R.S. (2007), "A review of transparent insulation systems and the evaluation of payback period for building applications", *Solar Energy*, Vol. 81 No. 9, pp. 1058-1071.
Wong, I.L., Eames, P.C. and Singh, H. (2008), "Predictions of Heating and Cooling Energy Demands for Different Building Variants with Conventional Building Fabric and Selected Fabric Interventions", *in: Proceeding of the Solpol 2008 – Renewable Energy: Innovative Technologies and New Ideas, Polish Solar Energy Society*, Warsaw, Poland, pp. 442-449.
Wong, I.L., Perera, R.S. and Eames, P.C. (2005), "A review of transparent insulation systems and the evaluation of payback period for building applications", *in Renewables in a changing climate, Innovation In Building Envelopes And Environmental Systems, Proceedings of CISBAT 2005, Lausanne, Switzerland*, Ecole Polytechnique Federale De Lausanne, Lausanne, pp. 65-70.

**Prefabricated TI-wall element**

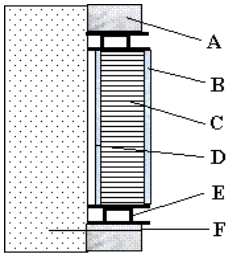


A) Opaque insulation;
B) Front cover glazing;
C) TIM;
D) Back glazing as absorber;
E) Metal or wood frame;
F) Massive wall with or without black paint

**Sealed TI-glazing**

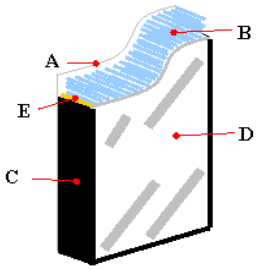


A) 5mm outside glazing;
B) 40mm acrylic glass capillary plate filled with rare-gas;
C) Gasket;
D) 4mm inside low-e glazing;
E) Spacer

Figure 1 Sketches of typical TI-wall and TI-glazing systems

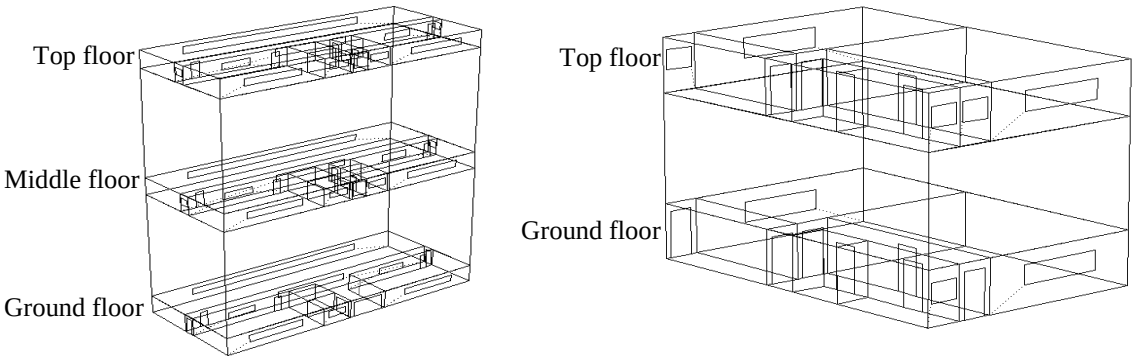


15-storey high-rise office building 4-storey low-rise office building

Figure 2 Wire frame drawings of the generic high-rise and low-rise office buildings indicating lower, intermediate and top floors

| Office Buildings | High-rise | Low-rise |
|---|---|---|
| Building floor plan | 35m x 15m | 15m x 10m |
| Building height | 15-storeys; 3m floor to floor height | 4-storeys; 3m floor to floor height |
| Floor areas | Ground floor: 525$m^2$<br>Upper floor: 7350$m^2$<br>Gross floor area: 7875$m^2$<br>Usable floor area: 7670$m^2$ | Ground floor: 150$m^2$<br>Upper floor: 450$m^2$<br>Gross floor area: 600$m^2$<br>Usable floor area: 585$m^2$ |
| External wall | Cavity wall: 2943$m^2$ | Cavity wall: 510$m^2$ |
| External windows | Double-glazed windows: 1536$m^2$ | Double-glazed windows: 85$m^2$ |
| Internal layout | Office space, conference room, emergency stairway and store rooms | |
| Building services | Artificial lighting, lift, centralised HVAC system to control heating & cooling, office equipment & appliances e.g. computers, copy machines, printers & fax machines. | |

Table 1 The design details and specifications of the generic high-rise and low-rise office buildings

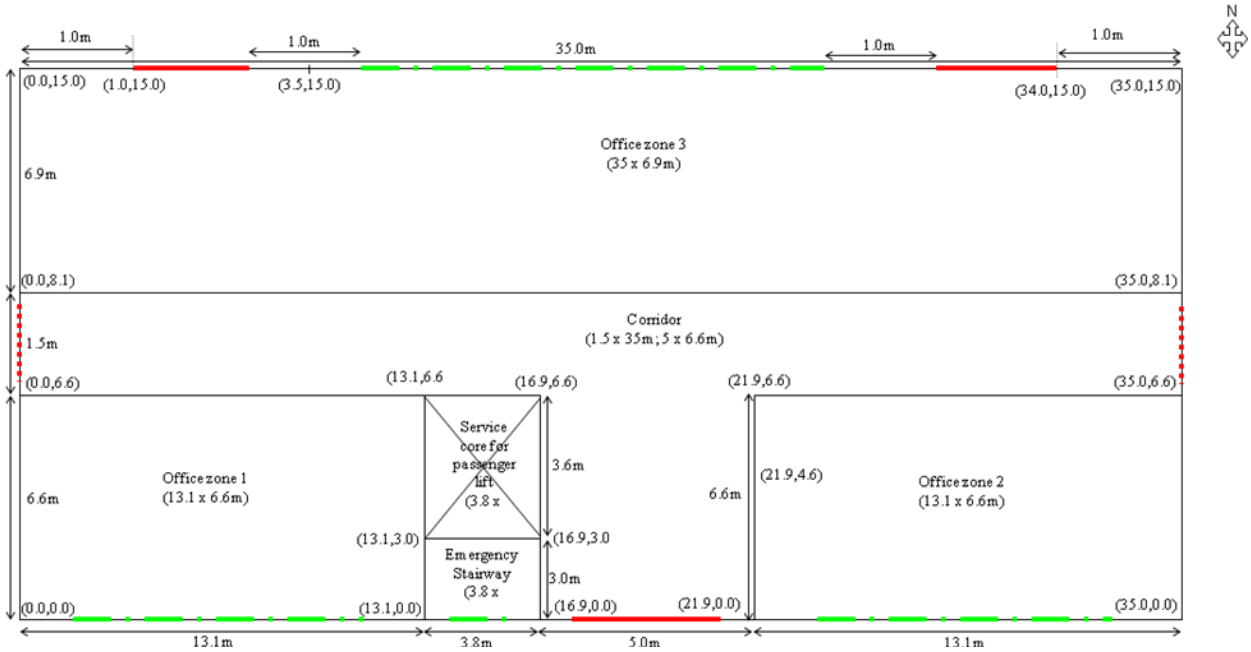


a) Ground floor layout plan

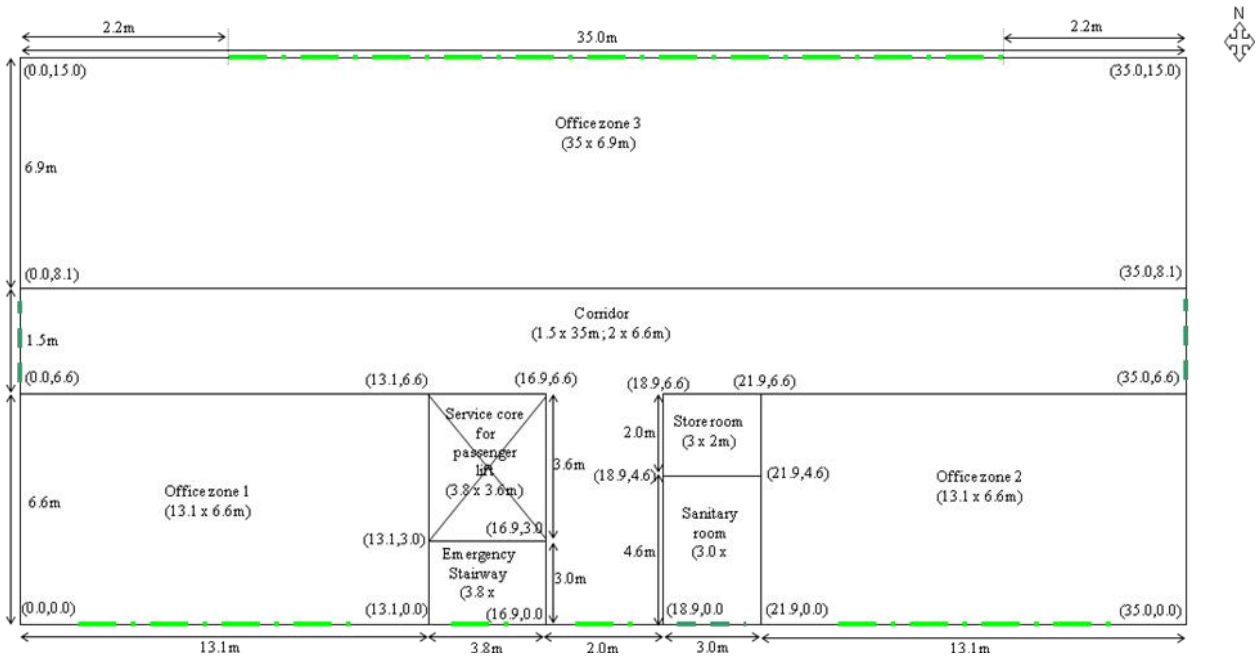


b) Upper floor layout plan (first to 14th floor)

Figure 3 Schematic ground and upper floor layout plan of the high-rise office building, with grid points

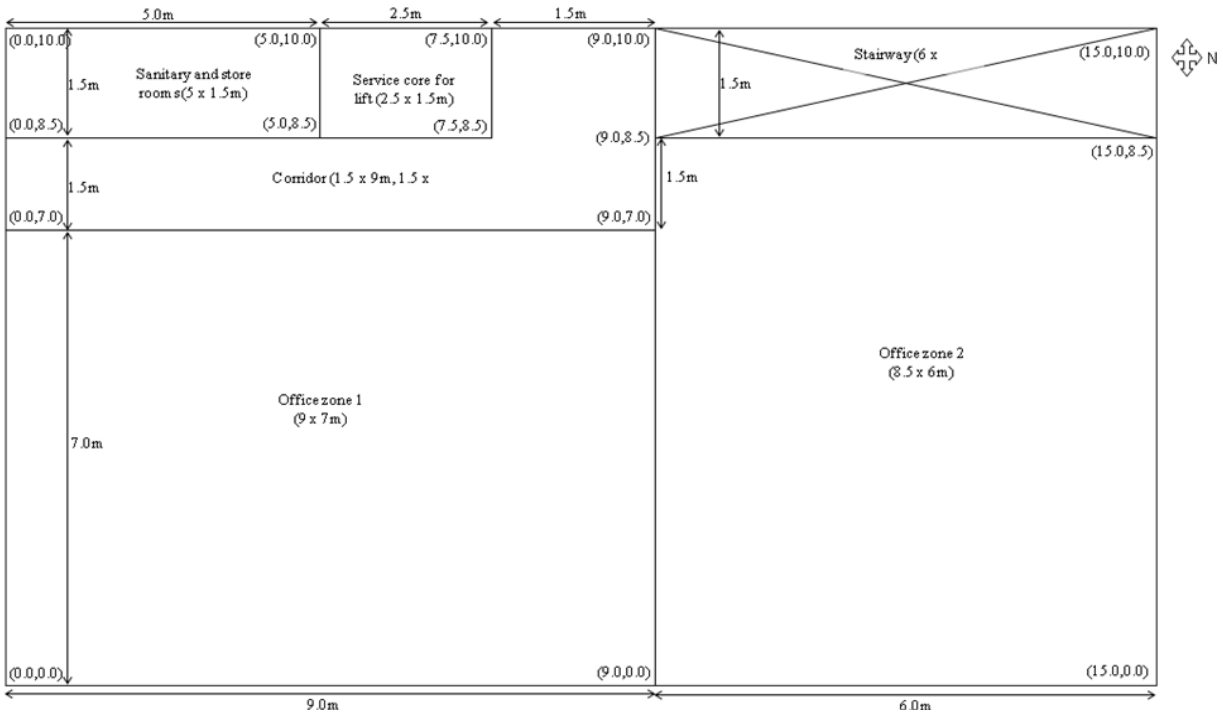


Figure 4 Schematic layout plan of the low-rise office building from the ground floor to the 3rd floor, with grid points

| High-rise Office Building | Name of Zones | | | Low-rise Office Building | Name of Zones | |
|---|---|---|---|---|---|---|
| | **G$^{rd}$ floor** | **7$^{th}$ floor** | **14$^{th}$ floor** | | **G$^{rd}$ floor** | **3$^{rd}$ floor** |
| Office zone 1 | GF-R1 | 7F-R1 | 14F-R1 | Office room 1 | GF-R1 | 3F-R1 |
| Office zone 2 | GF-R2 | 7F-R2 | 14F-R2 | Office room 2 | GF-R2 | 3F-R2 |
| Office zone 3 | GF-R3 | 7F-R3 | 14F-R3 | Corridor | GF-Cor | 3F-Cor |
| Corridor | GF-Cor | 7F-Cor | 14F-Cor | Lavatory | GF-Sani | 3F-Sani |
| Stairway | GF-Stair | 7F-Stair | 14F-Stair | Service core | GF-Lift | 3F-Lift |
| Service core | GF-Lift | 7F-Lift | 14F-Lift | Stairway | GF-Stair | 3F-Stair |
| Store room | | 7F-Store | 14F-Store | | | |
| Lavatory | | 7F-Sani | 14F-Sani | | | |

Table 2 Definition of zones for the high-rise and low-rise office buildings

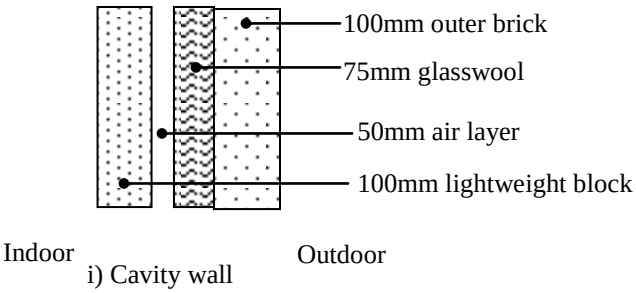


i) Cavity wall

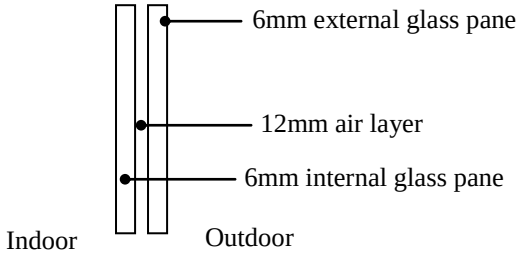


ii) Double-glazed windows

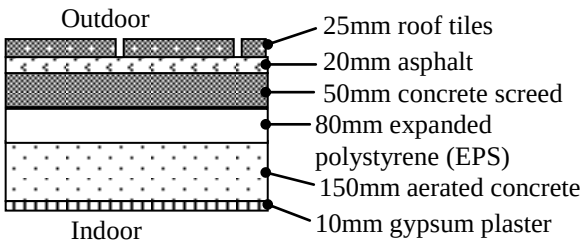


iii) Roof slab

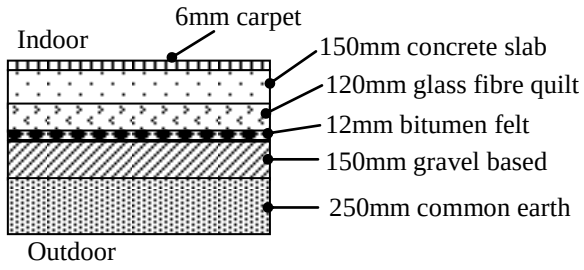


iv) Ground floor slab

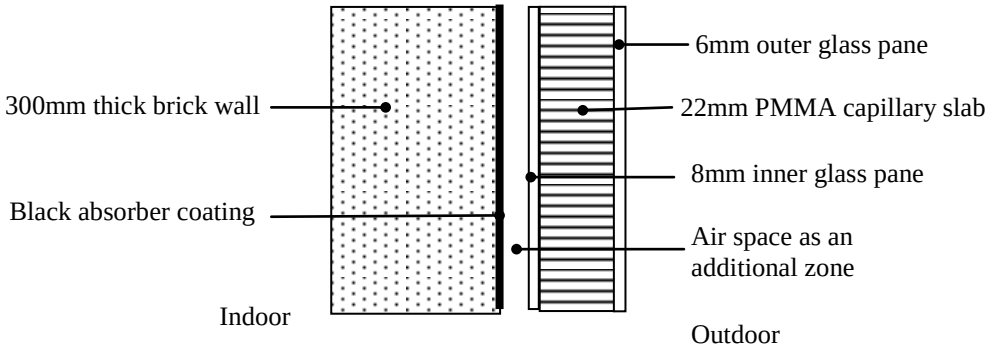


v) TI-wall system

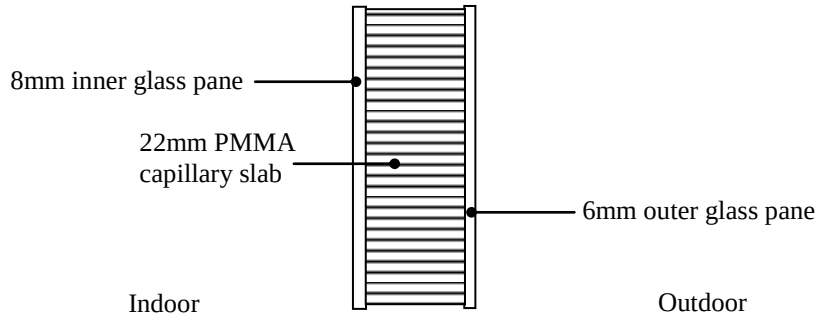


vi) TI-glazing system

Figure 5 Construction of conventional building envelope and the TI-facades used in office buildings

| Construction Details | Layers (outside to inside) | R-Value ($m^2K/W$) | Density ($kg/m^3$) | Specific heat capacity (J/kgK) | Thermal conductivity (W/mK) |
|---|---|---|---|---|---|
| Cavity wall | 100mm outer brick | 0.12 | 1700 | 800 | 0.84 |
| | 75mm glasswool | 1.88 | 250 | 840 | 0.04 |
| | 50mm air layer | 0.17 | 1.2 | 1.012 | 0.025 |
| | 100mm lightweight block | 0.53 | 1000 | 600 | 0.19 |
| Double-glazed window | 6mm glass pane | 0.01 | 2710 | 837 | 1.05 |
| | 12mm air gap | 0.17 | 1.2 | 1.012 | 0.025 |
| | 6mm glass pane | 0.01 | 2710 | 837 | 1.05 |
| Roof slab | 25mm roof tiles | 0.03 | 1900 | 800 | 0.84 |
| | 20mm asphalt | 0.04 | 1700 | 1000 | 0.50 |
| | 50mm concrete screed | 0.12 | 1200 | 840 | 0.41 |
| | 80mm expanded polystyrene | 2.67 | 25 | 1000 | 0.03 |
| | 150mm aerated concrete | 0.94 | 500 | 840 | 0.16 |
| | 10mm gypsum plaster | 0.02 | 1200 | 837 | 0.42 |
| Ground floor slab | 250mm common earth | 0.20 | 1460 | 879 | 1.28 |
| | 150mm gravel based | 0.29 | 2050 | 184 | 0.52 |
| | 20mm bitumen felt | 0.04 | 1700 | 1000 | 0.50 |
| | 120mm glass fibre quilt | 3.00 | 12 | 840 | 0.04 |
| | 150mm concrete slab | 0.13 | 2000 | 1000 | 1.13 |
| | 6mm carpet | 0.10 | 186 | 1360 | 0.06 |

| Construction Details | Layers (outside to inside) | R-Values ($m^2K/W$) | Density ($kg/m^3$) | Specific heat capacity (J/kgK) | Thermal conductivity (W/mK) |
|---|---|---|---|---|---|
| TI-glazing | 6mm clear float pane | 0.01 | 2710 | 837 | 1.05 |
| | 22mm PMMA slab | 0.55 | 30 | 1400 | 0.04 |
| | 8mm clear float pane | 0.01 | 2710 | 837 | 1.05 |
| TI-wall | 6mm clear float pane | 0.01 | 2710 | 837 | 1.05 |
| | 22mm PMMA slab | 0.55 | 30 | 1400 | 0.04 |
| | 8mm clear float pane | 0.01 | 2710 | 837 | 1.05 |
| | 20mm air gap | 0.17 | 1.2 | 1.012 | 0.025 |
| | 300mm wall mass | 0.36 | 2000 | 800 | 0.84 |

| **Angles of incidence** | **0°** | **40°** | **55°** | **70°** | **80°** |
|---|---|---|---|---|---|
| **1) KAPILUX System** | | | | | |
| Overall transmission | 0.691 | 0.402 | 0.308 | 0.130 | 0.017 |
| Absorption at: | | | | | |
| - 6mm external clear float pane | 0.016 | 0.018 | 0.019 | 0.020 | 0.021 |
| - 22mm PMMA slab | 0.138 | 0.485 | 0.570 | 0.737 | 0.931 |
| - 8mm internal clear float pane | 0.032 | 0.035 | 0.037 | 0.040 | 0.041 |
| **2) Double-glazed window** | | | | | |
| Overall transmission (visible transmittance of 0.76) | 0.611 | 0.583 | 0.534 | 0.384 | 0.170 |
| Absorption at: | | | | | |
| - 6mm external clear float glass | 0.157 | 0.172 | 0.185 | 0.201 | 0.202 |
| - 12mm air gap | - | - | - | - | - |
| - 6mm internal clear float glass | 0.117 | 0.124 | 0.127 | 0.112 | 0.077 |

Table 3 Thermo-physical and optical properties of building fabrics employed in the simulations

| | |
|---|---|
| 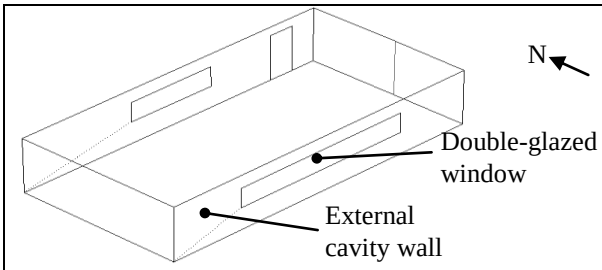 <br>a) office zone with external cavity wall and double-glazed window in high-rise office building (Case 1) | Case 1: 26.27m$^2$ cavity wall & 6.48m$^2$ double-glazed window |
| 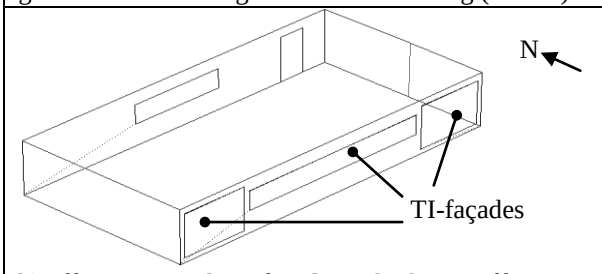 <br>b) office zone with TI-façades in high-rise office building (Cases 2, 3 and 4) | Case 2: 16.27m$^2$ cavity wall, 10m$^2$ TI-wall with 20mm air gap & 6.48m$^2$ TI-glazing<br><br>Case 3: 16.27m$^2$ cavity wall, 16.48m$^2$ TI-glazing<br><br>Case 4: 16.27m$^2$ cavity wall, 10m$^2$ TI-wall without 20mm air gap & 6.48m$^2$ TI-glazing |
| 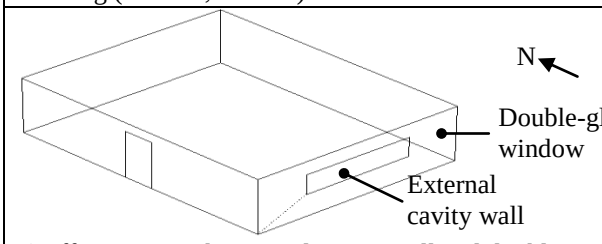 <br>c) office zone with external cavity wall and double-glazed window in low-rise office building (Case 1) | Case 1: 14.26m$^2$ cavity wall & 3.24m$^2$ double-glazed window |
| 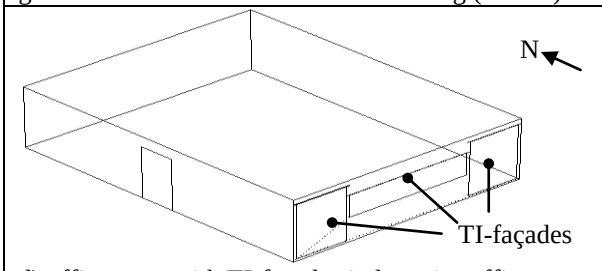 <br>d) office zone with TI-façades in low-rise office building (Cases 2, 3 and 4) | Case 2: 7.66m$^2$ cavity wall, 6.60m$^2$ TI-wall with 20mm air gap & 3.24m$^2$ TI-glazing<br><br>Case 3: 7.66m$^2$ cavity wall, 9.84m$^2$ TI-glazing<br><br>Case 4: 7.66m$^2$ cavity wall, 6.60m$^2$ TI-wall without 20mm air gap & 3.24m$^2$ TI-glazing |

Figure 6 Wire frame drawings of typical office zones for high-rise and low-rise office buildings for four different building envelope arrangements (Cases 1 to 4)

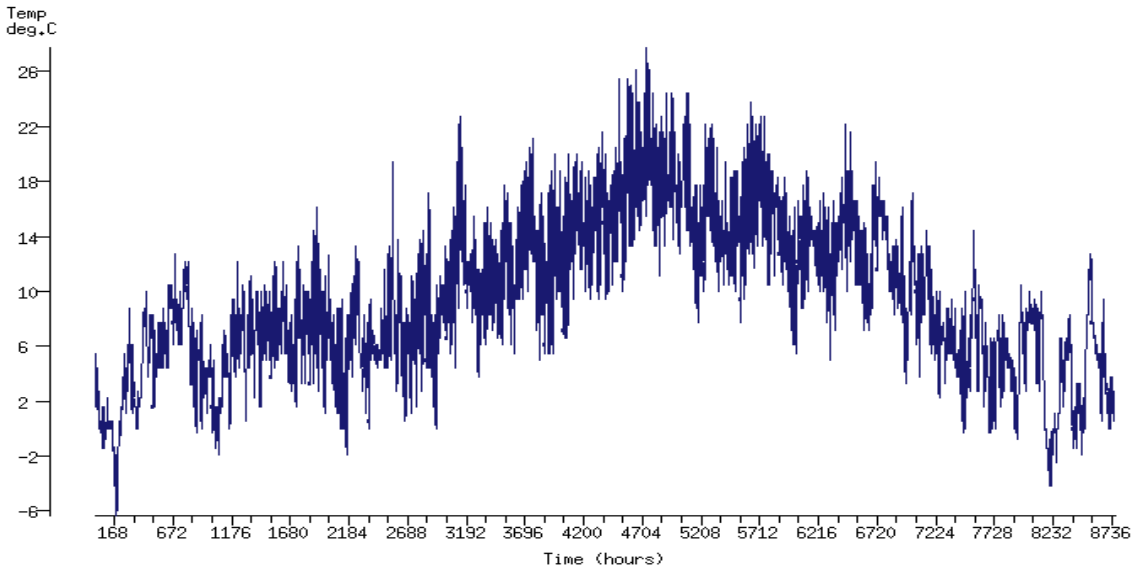

Figure 7 Typical meteorological year for dry-bulb temperature in London (latitude: 51˚30'N and longtitude: 0˚7'W)

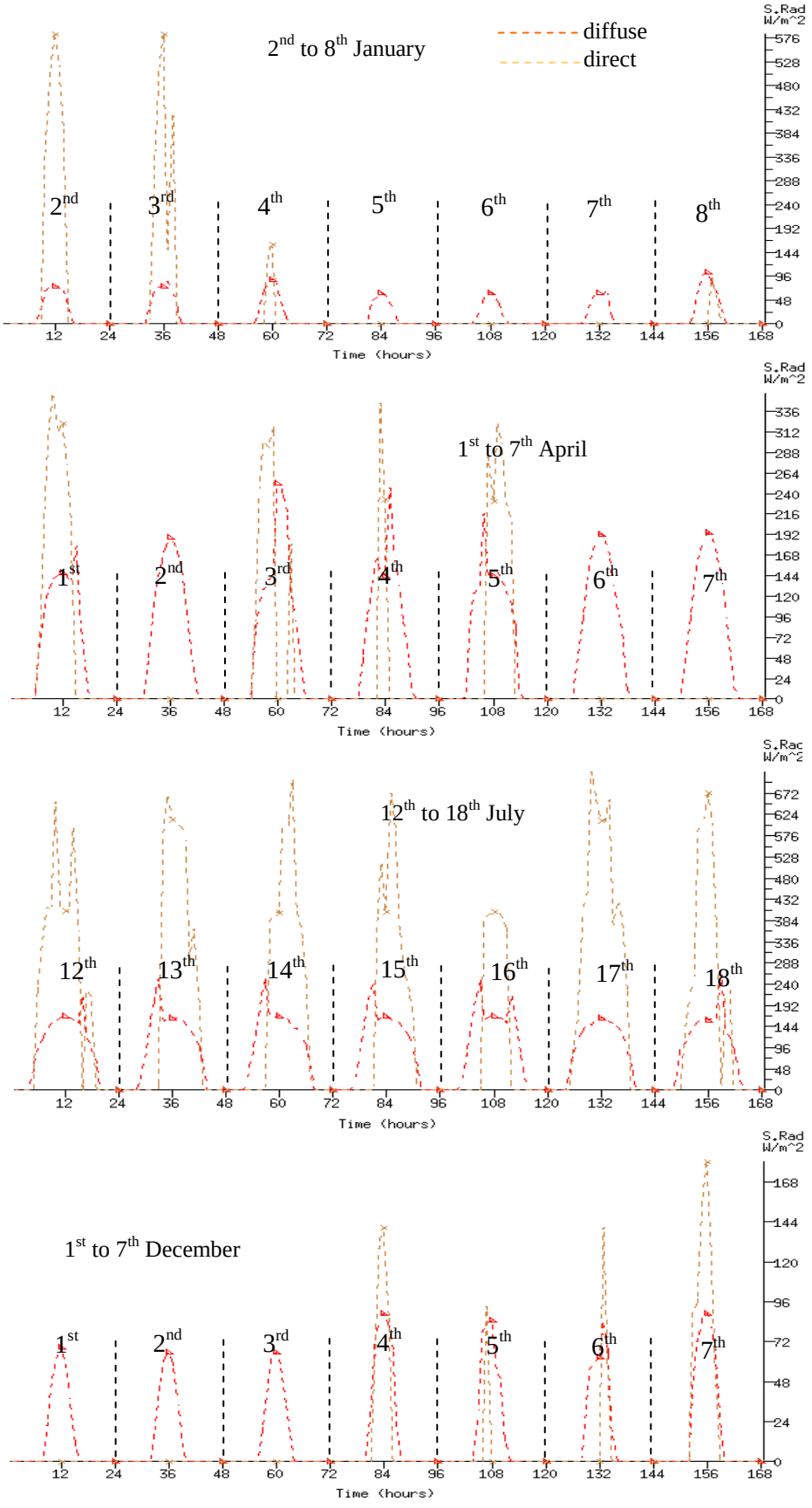


Figure 8 Direct and diffuse solar radiation (W/m$^2$) for London (51˚30'N; 0˚7'W)

| Day | Periods | System Control |
|---|---|---|
| Weekday (Mon-Fri) | 0000 to 0800 | Free floating |
| | 0800 to 0900 | Lower 15˚C heating and 24˚C cooling set points |
| | 0900 to 1700 | Maximum 20˚C heating and 24˚C cooling set points |
| | 1700 to 0000 | Free floating |
| Weekend (Sat-Sun) | All day | Free floating |

Table 4 Heating and cooling control parameters used for different periods in the office buildings

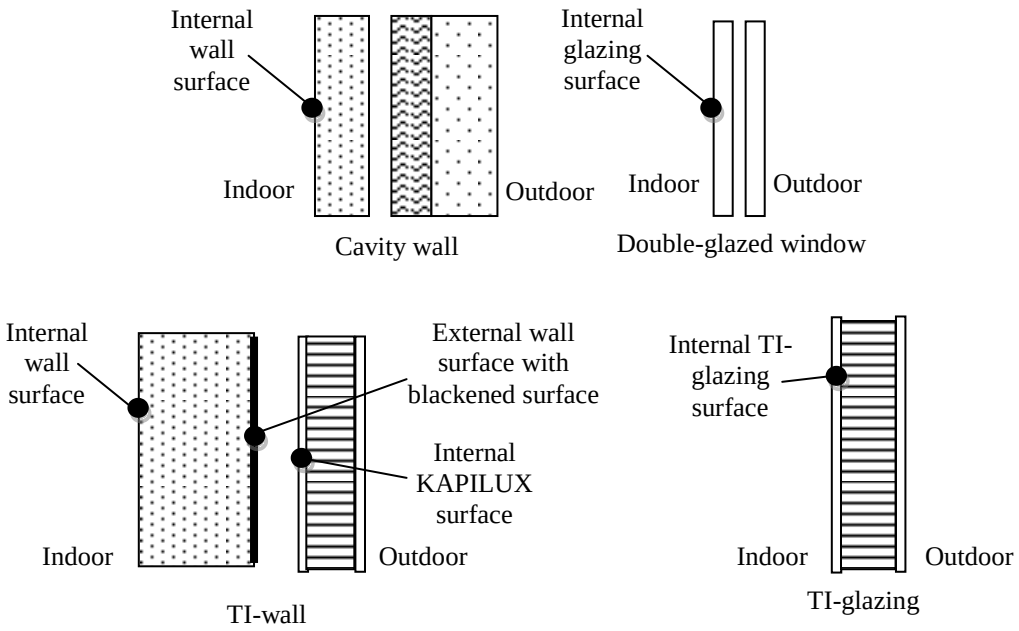


Figure 9 Sketches indicating the locations of the points in the façades (black dots) at which the surface temperatures were predicted

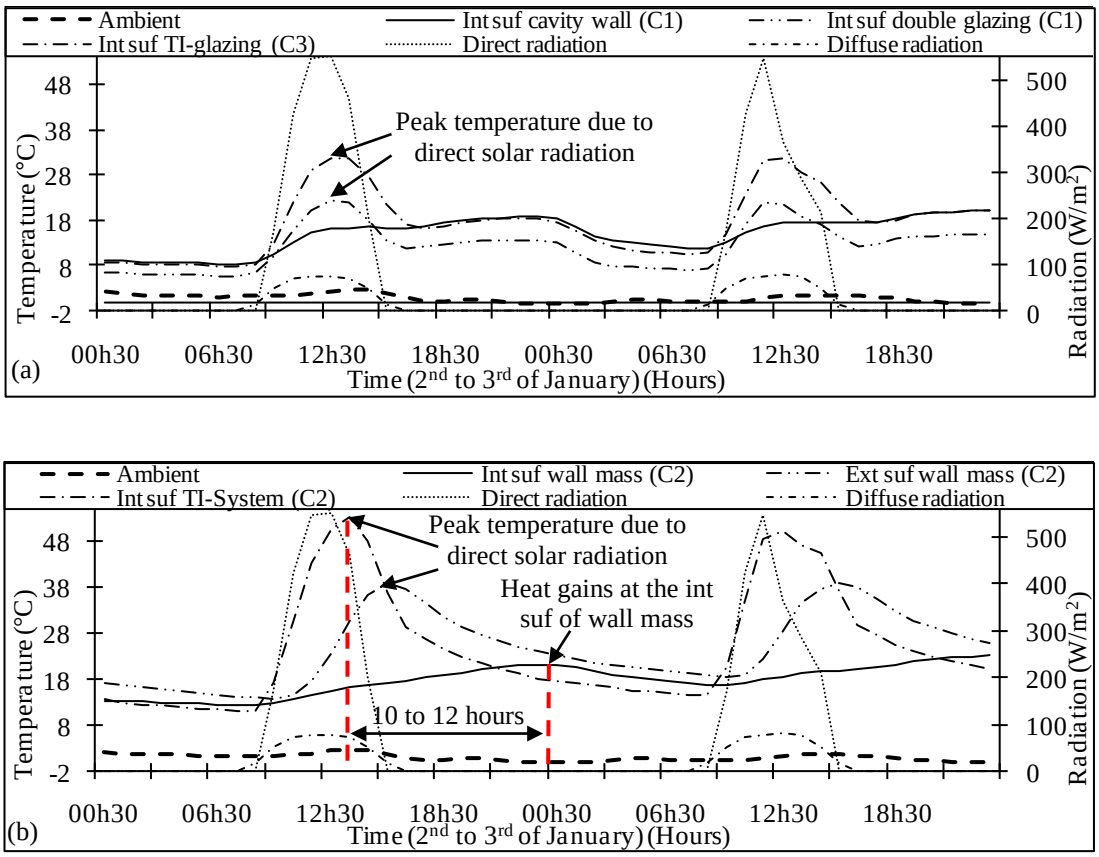


Figure 10 Internal and external surface (int suf and ext suf) temperature predictions for Case 1 (C1) to Case 3 (C3) in the high-rise (a & b) office building in winter in London

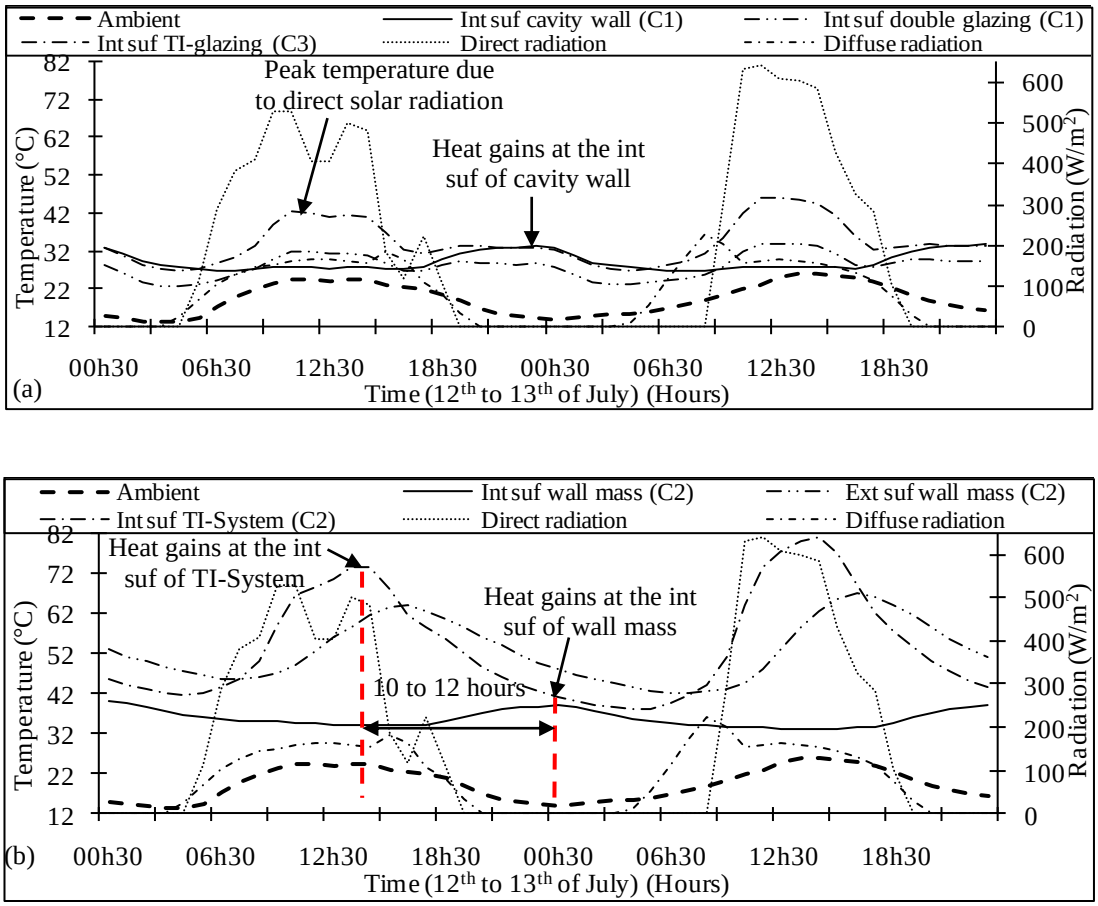


Figure 11 Internal and external surface (int suf and ext suf) temperature predictions for Case 1 (C1) to Case 3 (C3) in the high-rise (a & b) office building in summer in London

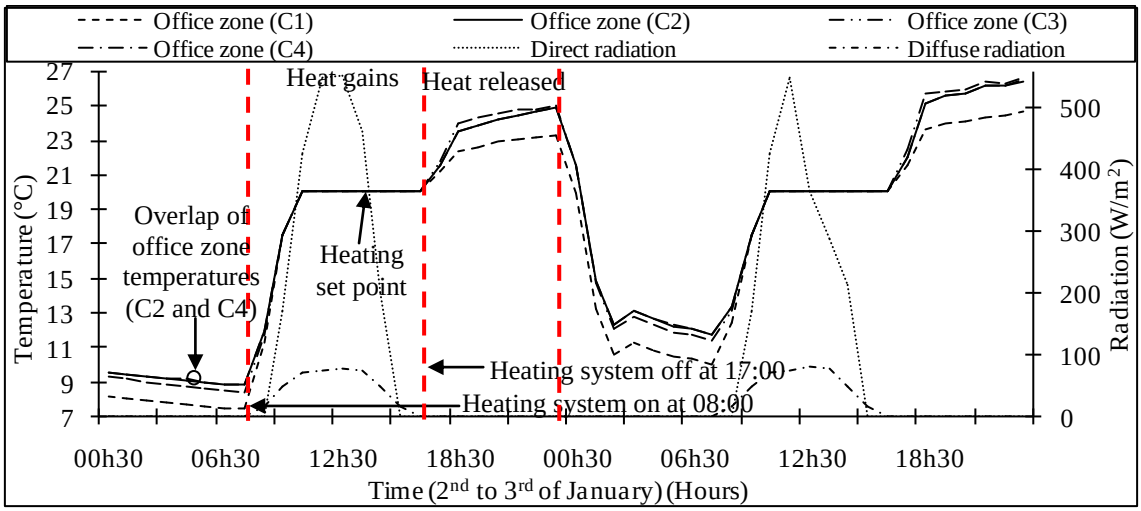


Figure 12 Zone temperature predictions for Case 1 (C1) to Case 4 (C4) in the high-rise office building in winter in London

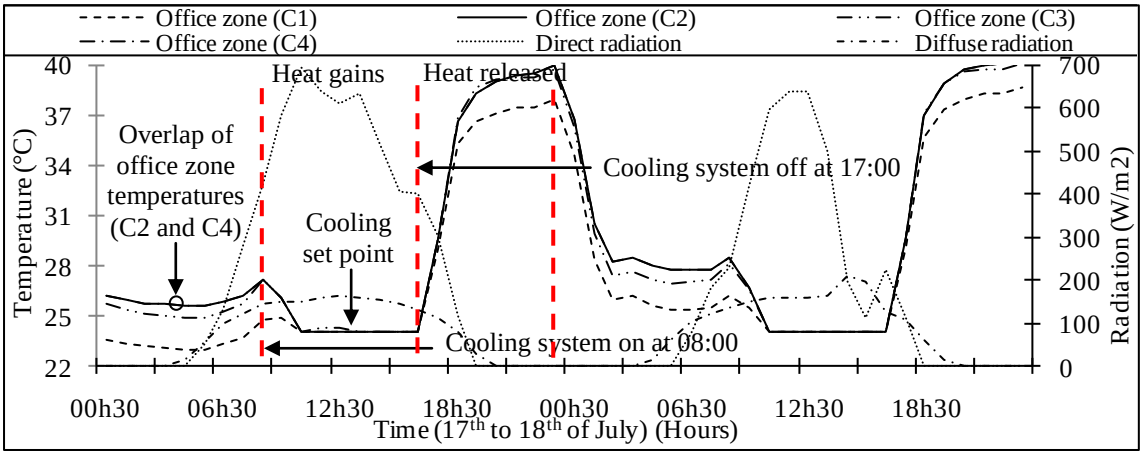


Figure 13 Zone temperature predictions for Case 1 (C1) to Case 4 (C4) in the high-rise office building in summer in London

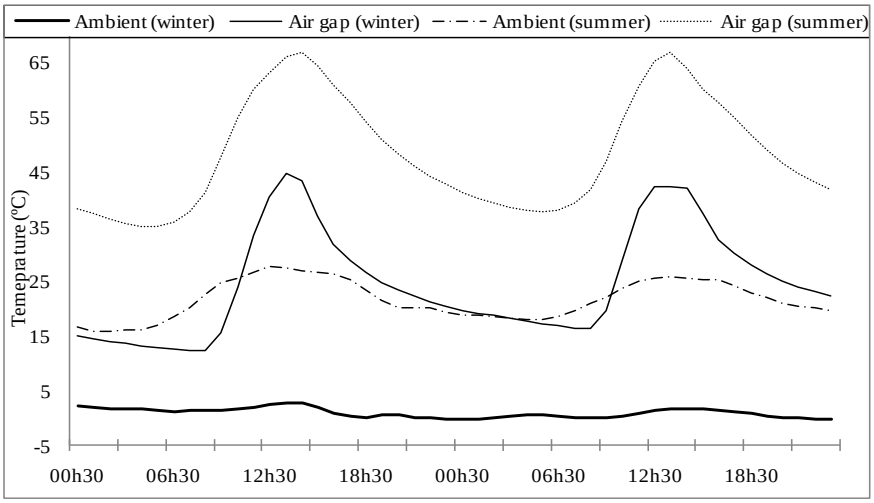


Figure 14 Predictions of ambient temperature and air gap temperature within TI-wall (Case 2) for winter (2nd and 3rd of January) and summer (17th and 18th of July) periods in London

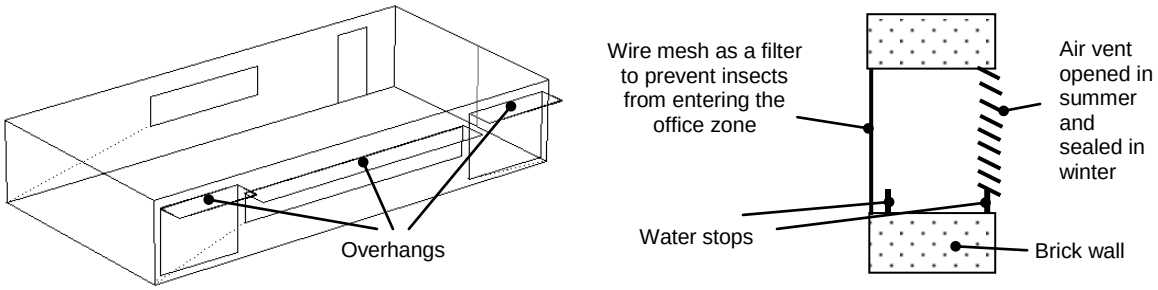


Figure 15 Illustration of overhangs and a typical air vent applied to the upper section of TI-systems in the south facing façades in the office buildings

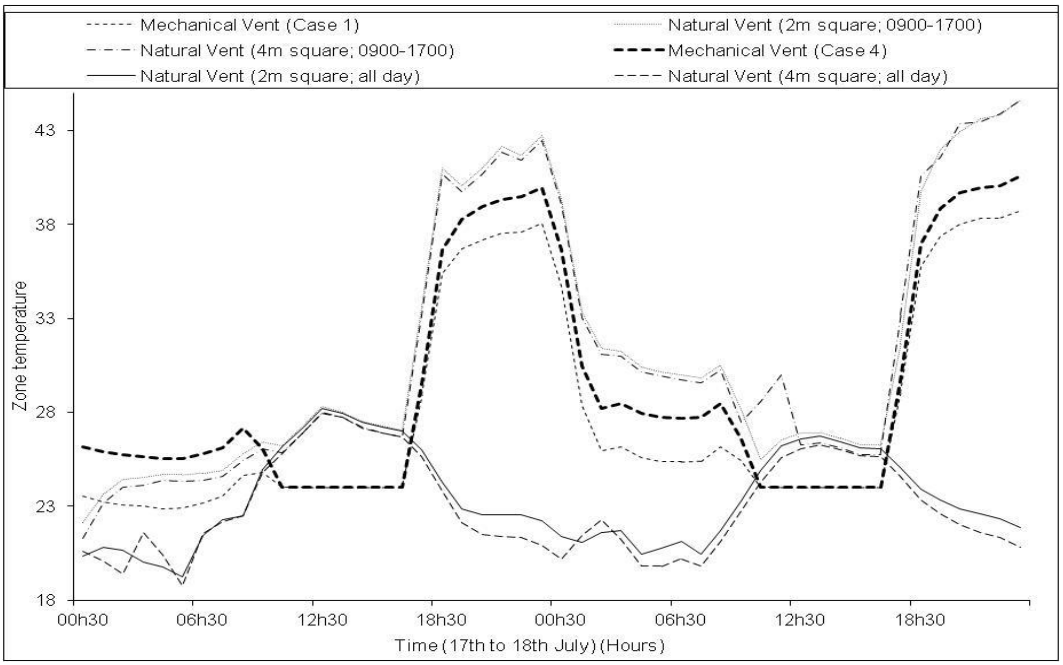


Figure 16 Comparison of air temperatures between naturally ventilated (Natural Vent) and mechanically ventilated (Mechanical Vent) office zone for the high-rise office building from 17$^{th}$ to 18$^{th}$ of July in London

| | Units | Case 1 | Case 2 | Case 3 | Case 4 |
|---|---|---|---|---|---|
| *High-rise office building* | $m^2$ | 7580 | 7580 | 7580 | 7580 |
| Heating energy demands | kWh | 354897 | 341954 | 338193 | 341668 |
| **Variations** | **%** | **Base case** | **-3.7** | **-4.7** | **-3.7** |
| Cooling energy demands | kWh | 59592 | 60033 | 60655 | 60033 |
| **Variations** | **%** | **Base case** | **+0.7** | **+1.8** | **+0.7** |
| Total energy demands | £ | 10236 | 10018 | 9984 | 10012 |
| **Variations** | **%** | **Base case** | **-2.1** | **-2.5** | **-2.2** |
| *Low-rise office building* | $m^2$ | 741 | 741 | 741 | 741 |
| Heating energy demands | kWh | 26044 | 25081 | 24461 | 25064 |
| **Variations** | **%** | **Base case** | **-3.7** | **-6.1** | **-3.8** |
| Cooling energy demands | kWh | 9040 | 9061 | 9101 | 9061 |
| **Variations** | **%** | **Base case** | **+0.2** | **+0.7** | **+0.2** |
| Total energy demands | £ | 1029 | 1012 | 1003 | 1012 |
| **Variations** | **%** | **Base case** | **-1.7** | **-2.6** | **-1.7** |

Table 5 Prediction of annual energy demands (both in kWh and £) for the office buildings in Cases 1 to 4 with 0.8 or 1m overhang application and all day natural ventilation in London